Target Concentration Dependence of DNA Melting Temperature on Oligonucleotide Microarrays

Ayse Bilge Ozel, Onnop Srivannavit, Jean-Marie Rouillard, and Erdogan Gulari
Dept. of Chemical Engineering, University of Michigan, Ann Arbor, MI 48109

DOI 10.1002/btpr.1505
Published online January 24, 2012 in Wiley Online Library (wileyonlinelibrary.com).

The design of microarrays is currently based on studies focusing on DNA hybridization reaction in bulk solution. However, the presence of a surface to which the probe strand is attached can make the solution-based approximations invalid, resulting in sub-optimum hybridization conditions. To determine the effect of surfaces on DNA duplex formation, the authors studied the dependence of DNA melting temperature (T_m) on target concentration. An automated system was developed to capture the melting profiles of a 25-mer perfect-match probe–target pair initially hybridized at 23°C. Target concentrations ranged from 0.0165 to 15 nM with different probe amounts (0.03–0.82 pmol on a surface area of 10^{18} A^2), a constant probe density (5×10^{12} molecules/cm^2) and spacer length (15 dT). The authors found that T_m for duplexes anchored to a surface is lower than in-solution, and this difference increases with increasing target concentration. In a representative set, a target concentration increase from 0.5 to 15 nM with 0.82 pmol of probe on the surface resulted in a T_m decrease of 6°C when compared with a 4°C increase in solution. At very low target concentrations, a multi-melting process was observed in low temperature domains of the curves. This was attributed to the presence of truncated or mismatch probes. © 2012 American Institute of Chemical Engineers Biotechnol. Prog., 28: 556–566, 2012
Keywords: DNA melting temperature, oligonucleotide microarray, target concentration, DNA hybridization thermodynamics

Introduction

DNA microarrays provide a means to screen and quantify thousands of nucleic acid sequences on a planar two-dimensional support simultaneously. Their increasing number of applications cover a wide range of fields. These include gene expression patterns of various organisms, genetic classifications, pathway mapping, pathogen detection, and the prediction of drug sensitivities and resistances, allowing for individualized and ultimately more effective medical treatments.[1–5]

With increasing interest in analyzing the genomic and transcriptomic characteristics of different biological entities, more questions began to arise in different stages of the process, going back to the fundamentals of DNA duplex formation reaction between an immobilized strand on the surface and a free one in solution. The factors that control nucleic acid hybridization in solution have been extensively studied.[6,7] However, as this reaction takes place on a solid–liquid interface in microarrays, the nature and characteristics of the surface gain importance in their individual contributions to duplex formation and dependence of melting temperature on its parameters.[8–12] These characteristics can be classified as individual design variables that can be manipulated for optimal experimental conditions: spacer length, nature/charge of the spacers; probe density, probe length, nature/charge of the probes; and nature/charge of the surface with respect to hybridization conditions. In addition, the presence of the denaturants as well as the concentrations of targets and salt in the hybridization solution would be expected to contribute to the equilibrium reaction, and therefore, affect the influence of the surface on the duplex formation.

Two of the main design problems that play a role in the accurate representation of the hybridization signal patterns on the surface come from false positive and false negative signals. False positive signals are mainly the result of cross-hybridization, which stems from the capture of targets that the probe is not designed for. Probe sequence design or low stringency of the hybridization conditions to discriminate the specific and nonspecific signals could lead to high background levels or miscalculation of fold changes in gene expression studies.[13] Although various posthybridization washing strategies have been devised to minimize this error, there are still recognizable problems with reproducibility[14] and brighter mismatch signals when compared with perfect matches.[15] On the other hand, false negatives are mainly due to low hybridization efficiency or insufficient hybridization by not allowing enough time to reach equilibrium, which could lead to underestimated signal intensities and, in turn, problems with estimating fold changes.[16] This is a common observation for genes with low expression levels,[17] which

Additional Supporting Information may be found in the online version of this article.

Current address of Ayse Bilge Ozel: Dept. of Human Genetics, University of Michigan, Ann Arbor, 1241 E. Catherine St., 4909 Buhl Building, Ann Arbor, MI 48109.

Correspondence concerning this article should be addressed to E. Gulari at gulari@umich.edu.

can also give rise to misidentification in genetic profiling.[18,19] Furthermore, the relative target concentrations and respective hybridization times in the experimental conditions become significant factors in the overall effect of false negative signals. Both of these situations seem to be due to the utilization of sub-optimal hybridization conditions given the characteristics of the surface and related solvent-mediated effects on DNA duplex formation. This makes it necessary to further explore how DNA would behave in a microarray environment under different conditions.

Recently, several investigations looking at the effect of different design parameters and their role in the thermodynamics and kinetics of the hybridization on the surface have emerged.[8,9,19–29] These theoretical and experimental studies conclude that binding thermodynamics and dependency of T_m could change due to the presence of the surface on which the probes are anchored. Thus, a limited capability exists for the current microarray and probe designs based on in-solution models utilizing the thermodynamic parameters and T_ms calculated using Nearest-Neighbor model, and the dependency of T_m on various variables such as sequence composition and arrangement; strand, ionic, and denaturant concentrations.[30] Nearest-Neighbor method, which is developed by SantaLucia Jr et al.,[7] takes into account the contextual orientations of the neighboring base pairs, and proposes that the stability of a base pair is contingent on the base-stacking contributions stemming from the interactions between these base pairs. Overall free energy, entropic, and enthalpic changes of the helix-to-coil transition and the melting temperature of a certain sequence can all be estimated using the values published for 10 possible base-pair combinations using the desired hybridization conditions.

The influence of strand concentrations (target concentration, probe density) on the duplex stability at a solid–liquid interface was investigated by Jayaraman et al. using Monte Carlo simulations.[31] These simulations concluded that as the surface becomes more crowded with increasing strand concentrations, the probability of binding to more than one strand increases, leading to additional entropic contributions affecting the duplex formation and its stability on the surface. In a similar study, Binder modeled the influence of the surface electrostatic and entropic changes on the binding affinity between a target strand in solution and a probe on the surface.[22] It was proposed that increasing the surface charge and decreasing the surface entropy would negatively influence the duplex formation on the surface. Since strand concentration can be one of the major contributors to these changes, it could be expected to have a similar result on the duplex stability on the surface.

Various kinetic studies have shown that the concentration of the target is one of the important parameters controlling the approach to equilibrium during hybridization (equilibrium time). In addition, it influences the equilibrium surface coverage and as a result, cross-hybridization, false-negative signals, and errors encountered in hybridization reactions.[14] However, based on the authors knowledge, apart from modeling studies, there is only one attempt at the experimental examination of the influence of target concentration on DNA duplex stability and its T_m on the surface by taking equilibrium into consideration.[8]

In this study, the authors present the results of their investigation of the mechanism of DNA hybridization on the surface by exploring the dependency of T_m on target concentration in an oligonucleotide microarray. Equilibrium melting curves were generated and analyzed at various target and probe concentrations. Experimental results regarding the equilibrium melting of a 25-mer perfect complementary DNA target–probe pair with different concentrations of target in solution and amounts of probe on surface (with a constant probe density) are presented.

Materials and Methods

Oligonucleotide arrays

The probe and the perfect complementary target of 25-nucleotide length were designed based on the sequence design criteria utilized by Owczarzy et al.[6] and SantaLucia Jr et al.,[7] with some modifications adapted for on-surface applications at the initial hybridization temperature of 23°C and salt concentration of 1 M NaCl. These include:

(1) The sequences are to be non-self-complementary.
(2) GC mole fraction of the sequences is to be between 0.2 and 0.8.
(3) No hairpins are present.
(4) Target–target dimer formation in solution, and probe–probe dimer formation on the surface are negligible when compared with perfect match probe–target formation on the surface.
(5) There are no long regions of GC and AT base pairs: no more than two triplet stretches, two doublet stretches, and three single stretches to reduce any nontwo-state behavior.
(6) The calculated-free energies are based on in-solution Nearest-Neighbor parameters,[7] and are to be as minimal as possible to create a stable structure at the hybridization conditions; keeping in mind that the instability imposed by the surface on the double-helix structure is unknown.

Several candidate sequences were designed using these criteria, and the following was randomly chosen from that list as the probe sequence:

5′-CGCGAGCACTGGACCGGTGTTGGGT-3′

The perfect complementary target in solution is labeled at the 3′ end with Cy5 fluorescent dye for detection, and the additional stability imposed by this dye moiety was assumed to be negligible for sequence design purposes.[32] The labeled target was purchased from IDT Technologies Inc (Coralville, IA) in PAGE purified form. The ozone susceptibility of Cy5 leading to degradation problems observed in hybridization studies[33] was minimized within the closed experimental system with minimum exposure.

The perfect-match probe sequence was synthesized on microfluidic chips, which were fabricated via photolithography,[34] and were comprised of seven channels connected in series in a serpentine fashion. In each channel, a set of 1000 sites was available for synthesis. Perfect-match probes (without any sequence variations), empty spots for background analysis and synthesis controls for intra-normalization were all randomly distributed along each channel to account for any possible concerns during synthesis and hybridization. For the same purpose, the first and the last channels included only the synthesis controls.

Synthesis controls were designed to monitor for the discrepancies in the system, and for the presence of any synthesis and hybridization defects as part of the quality control process. The synthesis control probes consisted of a 15-mer core probe sequence on the surface with corresponding perfect-match target of the same length labeled at the 3′ end with Cy3 fluorescence dye in the solution. The target was

Table 1. Summary of the Experiments Performed to Address the Effect of Target Concentration on the Duplex Formation on the Surface

Concentration of Target in Solution (nM)	Total Amount of Probe on Chip (pmol on C.S.A.*)	Target to Total Probe Ratio (pmol/pmol)
Experimental Set 1		
15	0.82	18.39 to 1
5	0.82	6.13 to 1
1.39	0.82	1.7 to 1
0.82	0.82	1 to 1
0.5	0.82	0.61 to 1
Experimental Set 2		
1	0.59	1.7 to 1
0.59	0.59	1 to 1
0.36	0.59	0.61 to 1
Experimental Set 3		
0.027	0.03	1 to 1
0.0165†	0.03	0.61 to 1

*C.S.A. = Chip Surface Area = 10^{18} Å^2. †Pre-hybridization at 50°C for 5 h.

purchased from IDT Technologies Inc. (Coralville, IA) in PAGE purified form. In addition to the sequential criteria mentioned above, both control target and probe sequences were designed to have negligible self–self hybridization and duplex formation with the main 25-mer probe and target sequences. Among the list of possible sequences created, the following was randomly selected as the perfect-match 15-mer control target sequence in solution:

5′-CTCCATACTAGTCAT-3′

Furthermore, for extra quality control, all different sequential combinations of 1–4 mers and random combinations of 5–10 mers were added at the 3′ end of the perfect complementary 15 mer control probe sequence on the surface. This created synthesis control probes of lengths 15–25 mers on the surface.

All probes were synthesized *in situ* on microfluidic chips in-house using previously developed β-cyanoethyl phosphoramidite chemistry incorporating light-directed addressable parallel synthesis in the 3′–>5′ direction.[35] The glass–silicon chip surface was first derivatized with *3-aminoproplytriethoxysilane* linker (Gelest, Morrisville, PA). Next, a spacer consisting of 15 dT was synthesized on the linker's amine group, followed by the light-directed synthesis of the randomly distributed main and control probes.

Experimental design and set-up

The experimental design to study the effect of target concentration on T_m consisted of three separate sets, each having a different probe amount with a constant probe density of 5 × 10^{12} molecules/cm^2 on a chip surface area of 10^{18} Å^2. The probe density was estimated and reported in a previous study.[36] The total amount of probes in Experimental Set 1 was 0.82 pmol/10^{18} Å^2; in Experimental Set 2, it was 0.59 pmol/10^{18} Å^2; and in Experimental Set 3, it was 0.03 pmol/10^{18} Å^2. The probe density was constant in all sets, and the total amount of probe was controlled by the number of synthesis spots. More specifically, there were 3,900 spots for probes in Experimental Set 1; 2,800 spots in Experimental Set 2; and 145 spots in Experimental Set 3. These perfect-match probe spots were randomly distributed along the channels. These three experimental sets are summarized in Table 1. All experiments were run under the exact conditions as described in the Section "Hybridization and Generation of Melting Curve Profiles," while keeping the solution conditions, target, and probe sequences the same across all sets.

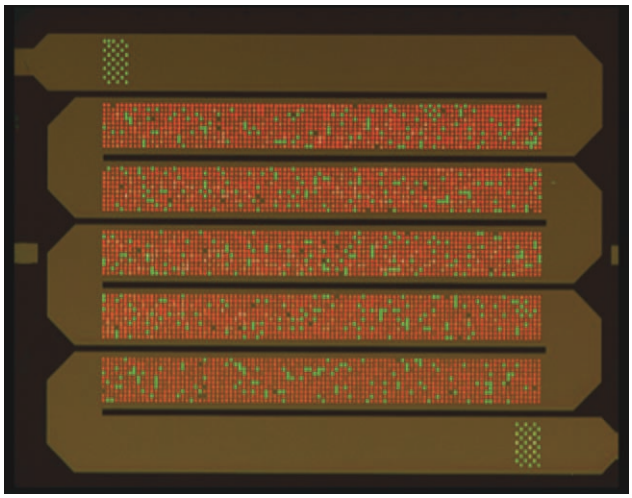

Figure 1. A microfluidic chip hybridized with the target (red) and control (green) sequences.

The experimental set-up was an in-house designed system, which included a holder fitting into the scanner with the appropriate fluidic and electrical connections for fluid and temperature control, a temperature controller, a micro pump, a computer, and a fluorescence laser scanner (See Supporting Information Figure S1). The temperature intervals and increments were fed into the system via an interface embedded into GenePix Pro 4.0 Software (Molecular Devices, Sunnyvale, CA), and equilibrium times were input into a separate in-house Java program called by this interface. The microfluidic chip was scanned automatically at each temperature when equilibrium was reached with the settings determined by the user, and the image was recorded (Figure 1). The fluorescence signal intensities from these images were later extracted.

Hybridization and generation of melting curve profiles

The hybridization was carried out at 23°C with 1000 μL hybridization solution consisting of Cy5 labeled main target at designated concentrations, 15 nM Cy3 labeled control target, and 0.1 μg/μL acetylated BSA in 6× SSPE buffer (1 M NaCl, 0.07 M Na_2HPO_4, 7 mM EDTA) at pH 6.7. This solution was constantly re-circulated through the microfluidic chip at 500 μL/min, and the equilibrium state was determined by negligible Cy5 fluorescence signal intensity variation on the perfect-match probes measured with the Axon 4000B fluorescence laser scanner (Molecular Devices, Sunnyvale, CA) at determined (near saturation) PMT voltage values in the excitation wavelengths of 532 nm (Cy3 dye, green channel) and 635 nm (Cy5 dye, red channel).

Melting curve profiles were generated by acquiring the fluorescence signal intensity over a determined temperature range, a heating rate, and equilibration time at each temperature step (See Supporting Information Figure S2). The temperature range was set from 23 to 85°C due to the experimental set-up restrictions. Initial hybridization at 23°C took between 1 and 4 h contingent on the target concentration. The heating rates and the corresponding equilibration times were set based on the temperature and the observation of equilibrium at that temperature with the re-circulating

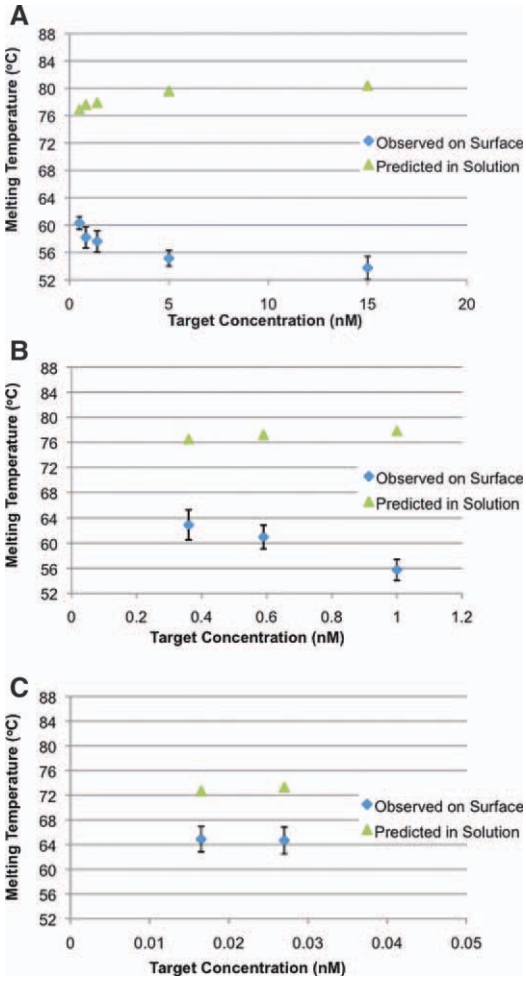

Figure 2. The melting temperature trends observed on the surface and predicted in solution (using Nearest-Neighbor method) with respect to different target concentrations at perfect match probe amounts of 0.82 pmol (A), 0.59 pmol (B), 0.03 pmol (C) on 10^{18} Å^2 surface.

hybridization solution. Therefore, the heating rate below 65°C was 3–5°C/h, and above 65°C, it was 5–10°C/h. Equilibration times ranged between 1 and 45 mins, depending on the temperature and the target concentration.

Data analysis

The quality of the synthesized chips was initially verified by checking the spot size for 50 μm diameter and the uniformity on the spot cross-section. The main quality assessment and intra-normalization were carried out using the synthesis control signals obtained at the initial hybridization temperature of 23°C. The signal intensities of control probes in each channel were analyzed separately with respect to their lengths from 15 to 25 nt. All of the distributions were tabulated together and the ratios were taken with respect to a given channel on the chip at each length. The averages of these ratios were used in the intra-normalization process in the red channel based on the lowest of the average of the ratios in the green channel.

The normalized red channel signals, which resulted from hybridizing targets on the surface, were further analyzed by customized Matlab code (Natick, MA) for faster processing. The analysis in Matlab included: background signal correction of the probe sites; temperature calibration of these fluorescence signals; smoothing and fitting of the experimental melting curve obtained at each spot; extraction of the melting temperatures and finally, statistical analysis. Background signal correction and temperature calibration of the probe signals were made using the empty spot signals at each temperature. Smoothing was carried out using the Savitzky–Golay method,[37] and the experimental curves were fitted with a representative sigmoidal function, Boltzmann equation with characteristics of the melting process being represented by its individual parameters: the dynamic range of operation (a_1–a_2), the melting point (x_0) and the extent of curve broadening due to the surface effects (dx):

$$\text{Signal Intensity} = a_2 + \frac{(a_1 - a_2)}{1 + \exp\left(\frac{(x - x_0)}{dx}\right)} \qquad (1)$$

where x is the temperature, a_1 is the highest signal intensity, and a_2 is the lowest signal intensity. Lower and upper baselines were established from the linear regions before and after the transition using the new algorithm for selection of linear sloping baselines as proposed by Owczarzy.[37] The melting temperatures recorded from the inflection points of each of these curves (where the fraction of duplexes is equal to 0.5) were tabulated along with R-squared fit of the equation to the experimental data. R-squared values lower than 0.98 were considered to be bad fits, and the remaining melting temperature values were analyzed for outliers for each probe.

Results and Discussion

Perfect match probes, synthesis controls, and the empty spots were randomly distributed and replicated on each chip for reproducibility. There were 3,900, 2,800, and 145 perfect-match probe spots in Experimental Sets 1, 2, and 3, respectively, which determined the amount of probes on the surface at the constant probe density. The normalized average net signal intensities of these probes at the hybridization temperature showed uniformity in all the experiments with on-chip variations within 2–5% of the average signals. Accordingly, the authors were able to obtain highly reproducible and reliable melting temperatures with standard deviations between 0.5 and 2% of the average calculated values after the analysis was complete. Since statistically, ~97.5% of the probes demonstrated an R-squared curve fit >0.98 in each experiment, it can be concluded that the reported melting temperature values on each chip are accurate representations of the DNA behavior on the surface in this experimental system. Furthermore, a comparison of the analysis method performance with the commonly used melting temperature extraction method utilizing the duplex fraction vs. temperature curves yielded values as different as 1.2°C (not shown). This is within the experimental and analysis error limits of both methods, showing the precision of the equation used for the curve fit in the analysis.

Decreasing DNA melting temperatures with increasing target concentrations at all probe concentrations

Figure 2 shows the melting temperature trends observed on the surface in comparison with the predicted in-solution

melting temperatures. These predictions were made using the Nearest-Neighbor method[7] for each experimental set presented in Table 1. It estimates the melting temperature by utilizing the three sets of thermodynamic parameters (the free energy change, the enthalpy change, and the entropy change) published for 10 possible base-pairs.

In Figure 2A, it is observed that the change in target concentration from 0.5 to 15 nM with a probe amount of 0.82 pmol on a surface area of 10^{18} Å^2 results in a 6°C decrease in on-surface T_m, compared with a 4°C increase in in-solution T_m. Similarly, in Figure 2B, when the target concentration was increased from 0.36 to 1 nM with a probe amount of 0.59 pmol on the same surface area, the decrease in on-surface T_m is 7°C compared with a 2°C increase in in-solution T_m. Moreover, in Figure 2C, which demonstrates the data points at the lowest target concentrations used (0.027, 0.0165 nM), the increase in on-surface and decrease in in-solution T_ms are comparably very small. Two possible explanations could be that the measurements are at the minimal detection level of the system, and therefore, these trends may not be clearly observed; or the limit of concentration dependence might have been reached at these concentrations.There are two main observations that can be deducted from these plots:

• *All observed melting temperatures on the surface are lower than predicted in-solution melting temperatures.*

Melting or denaturation of a DNA duplex is a thermodynamic process in which the main contributing forces holding the structure together, namely hydrogen bonding and base-stacking, are disrupted and broken. Denaturation of the helix structure can be accomplished with different physical factors, such as salt and denaturant concentrations, pH, or heat by increasing the medium temperature. Depending on the stability of the duplex, these parameters would impact the helix-to-coil transition differently. In solution, these factors can affect both strands similarly without any interference from the neighboring duplexes or surfaces under certain conditions.[38]

However, on microarrays, additional interactions or factors seem to affect these reactions.[39] In a situation where one of the strands is immobilized on an impenetrable wall in a dense layer, the interactions with the adjacent single strands or duplexes, the distribution of ions within and close by the layer, and the presence of the surface itself can not be disregarded. The contributions of these components could potentially play a significant role in reducing the stability of the DNA duplex formed on the surface,[10,28] which in turn, is reflected in the decreased melting temperature when compared with in-solution.[40]

The decrease in the stability of the duplex with respect to in-solution may be attributed to the electrostatic and entropic blocking of the surface. As the hybridization takes place on a charged solid–liquid interface with a charged layer of spacers and probes, an electrostatic blocking could be imposed on the hybridizing targets by these layers.[22] Moreover, the immobilization of one of the strands, the impermeability of the wall, and the increasing crowding within the probe layer may also make it comparably less favorable for the free targets to hybridize with the probes on the surface. Namely, the entropic blocking can act as another dominant factor in creating an additional penalty on duplex formation.[10,12,22]

The authors findings are in general agreement with these studies that a lower DNA stability and melting temperature could be expected on the surface when compared with in-solution.

• *In all experimental sets, an increase in target concentration is accompanied with a decrease in melting temperature observed on the surface.*

Commonly used as a stability indicator, DNA melting temperature is a quantity that is highly dependent on the concentration of the strands. It is expected in solution that denaturation of 50% of duplexes would be observed at a higher temperature (T_m) when the concentration of the duplexes is higher at the initial hybridization temperature.[41] However, on microarrays, the presence of a surface and immobilization of one of the strands can alter the thermodynamics and kinetics of duplex formation and the dependence of T_m on its parameters.[39] Due to their similarity to homogeneous liquid–phase reactions, gel-based arrays perform almost identical to in-solution reactions,[42] i.e., an increase in target concentration would yield increasing DNA melting temperatures.[43] Nevertheless, in this study, the authors experimental observations on the heterogeneous solid-phase hybridization reaction on an oligonucleotide microarray suggest that there could be an unfavorable effect of the surface electrostatics and static hindrance, resulting in an opposite T_m trend compared with in-solution and gel-based array expectations.

In agreement with the results presented by the simulations and models by Jayaraman et al.[31] and Binder,[22] an increase in the target concentration seems to inversely influence DNA duplex stability on the surface. In their modeling study, Jayaraman et al. investigated the effect of target concentration and probe density on the thermodynamics of hybridization using Monte Carlo simulations. It was observed that when a higher target concentration or probe density was used in the experiment (in other words, higher strand concentrations), the probability of the target binding to more than one probe also increased. This would lead to additional configurational entropy restraints on the duplexes formed, making the structure less stable, and thus lowering the melting temperature. A similar conclusion is reached in the modeling study by Binder, who looked at the effect of target concentration on the surface adsorption of the target to the oligonucleotide probes attached on the surface as a part of the investigation. This different approach modeled the affinity between the target strand in solution and the probe on the surface by taking into account the changes in the surface charge (electrostatic blocking) and entropy (entropic blocking) as more and more duplexes form on the surface. It was suggested that any condition increasing surface charge and decreasing entropy would inversely influence the duplex formation on the surface, and an increase in target concentration could be considered one of these conditions.

As part of their study, Forman et al.[8] experimentally investigated the influence of target concentration on hybridization and melting of DNA duplexes on the surface. Affymetrix GeneChip® arrays with 10–20 mer probes were hybridized with a 20-mer complementary target with target concentrations ranging from 1 to 500 nM. The probe array was continually exposed to a constant concentration of target solution, and melting curves were generated with increasing temperatures at 5°C intervals, with a 30-min equilibration time at each temperature point. This study arrived at a different conclusion that the target concentration did not seem to have an effect on T_m. Unlike the authors study, the sensitivity in melting curve generation was rather low. Saturating

densities were also indicated to be reached at less than 10% of the probe density, indirectly pointing out the surface saturation capacity of the target concentrations used in their experimental conditions. Moreover, with their given synthesis step-wise yield of 90%, full length population of the probes would be as low as 40% and 15% for 10 and 20 mer probes, respectively; leading to a highly heterogeneous population of truncated probes. Therefore, the melting curves and temperatures obtained would represent the melting process of high population of these truncated probes.

Proposed models to investigate the experimental hybridization patterns at the surface–liquid interface commonly rely on the Langmuir adsorption model.[44–47] In its simplest form, the Langmuir model relates the fraction of occupied probe sites at various target concentrations at a specific temperature. Limitations of this model, which include the inherent interactions and nonsimilarities between probe sites, have prompted different extensions, which has been taken into account factors such as competitive hybridization.[22,48] While interpreting the observed results to a certain degree of accuracy in some of the studies at constant temperature,[44–47] this method seems to represent a partial view of the overall picture by not considering the effects of temperature on the reaction thermodynamics, equilibrium, and kinetics. Multiple experiments at various temperatures and target concentrations can be utilized to broaden the interpretations of this approach; however, to the best of the authors knowledge, to date, there have been no published models directly relating the target concentration to melting temperature on the surface, while implementing the effects of temperature on the thermodynamic parameters.

In this study, the authors present a combined thermodynamic and kinetics approach to bring an understanding to the observed T_m trend with respect to target concentration.

Depending on the conditions imposed, the hybridization efficiency would be influenced by the presence of the surface. There are certain cases in which the maximum surface coverage, which is a direct indication of the equilibrium conversion, can be lower than 0.1.[28] This indicates that the in-solution T_m definition needs to be adapted for on-surface applications. Therefore, a new parameter, m, is introduced to describe the maximum surface coverage achieved at the initial hybridization temperature at equilibrium. The melting temperature of DNA on the surface is then observed at a duplex fraction of $0.5 \times m$. According to this new definition, the hybridization process on the surface can then be expressed as:

	T	+	P	$\Leftrightarrow$	TP
initial	T_0		P_0		
reacting	$-\theta m P_0$		$-\theta m P_0$		$+\theta m P_0$
final	$T_0 - \theta m P_0$		$P_0(1-m\theta)$		$\theta m P_0$

where the initial probe concentration, P_0, is the limiting reactant, and the target concentration, T_0, as in most cases, is in large excess. The hybridization efficiency at the end of the process is $\theta \times m$, and is equal to 1 when all of the probes are available for the duplex formation, as in the case of most in-solution reactions.

The association equilibrium constant of this reaction can be formulated as:

$$K_a(T) = \frac{[TP]}{[T]\times[P]} = \frac{P_0 m\theta}{(T_0 - P_0 m\theta)\times P_0(1-m\theta)} \quad (2)$$

at any temperature, which becomes,

$$K_a(T_m) = \frac{m\times 0.5}{(T_0 - P_0 m\times 0.5)\times(1-m\times 0.5)} \quad (3)$$

at the melting temperature of the duplex, where $\theta = 0.5$.

Knowledge of the maximum extent of hybridization, m, and the initial target-to-probe concentration ratio, T_0/P_0, is required to calculate the association equilibrium constant at the desired duplex fraction. Obtaining these values at the initial hybridization temperature will allow the authors to compare the stability of a duplex formed on the surface with the one in solution through the relationship between the association equilibrium constant and the free energy change of duplex formation at the standard temperature:

$$\Delta G^0 = -R\times T\times \ln(K_a) \quad (4)$$

Even though the values of m and the real T_0/P_0 on the surface were unknown, an attempt was made to relate the equilibrium constants at the melting and initial hybridization temperatures through various thermodynamic relationships, and observe how different values of m and initial target-to-probe concentration ratio would affect the melting temperature; with the initial hybridization temperature set constant to 23°C, as was in the experiments.

For systems at constant pressure and temperature, change in the Gibbs free energy of reaction can be expressed as[49]:

$$\Delta G^0 = \Delta H^0 - T\times\Delta S^0 \quad (5)$$

where ΔH^0 is the standard enthalpy change of reaction and ΔS^0 is the standard entropy change of reaction at the reference temperature (T_0). Recent studies have shown that for in-solution duplex formation reactions, the enthalpy and entropy changes are temperature dependent.[50] This temperature dependency can be incorporated into the equation by including the specific heat capacity change, $\Delta C_p{}^0$, and combining the terms to obtain the temperature-dependent van't Hoff equation:[49]

$$\frac{\Delta G^0(T)}{RT} = \frac{\Delta G^0(T_0) - \Delta H^0(T_0)}{RT_0} + \frac{\Delta H^0(T_0)}{RT} + \frac{1}{T}\int_{T_0}^{T}\frac{\Delta C_p^0}{R}dT - \int_{T_0}^{T}\frac{\Delta C_p^0}{R}\frac{dT}{T} \quad (6)$$

The specific heat capacity change can be assumed to be independent of temperature.[51] After the integrations are carried out, the relationship between the association equilibrium constant and the free energy change (Eq. 4) can be incorporated into the van't Hoff equation at any temperature:

$$\Delta G^0(T_0) = RT_0\times \times\left[-\ln K_a(T) + \frac{\Delta H^0(T_0)}{R}\left(\frac{1}{T_0}-\frac{1}{T}\right) - \frac{\Delta C_p^0}{RT}(T-T_0) - \frac{\Delta C_p^0}{R}\ln\left(\frac{T}{T_0}\right)\right] \quad (7)$$

The standard Gibbs free energy change at the standard temperature (T_0) will be the same at the initial hybridization

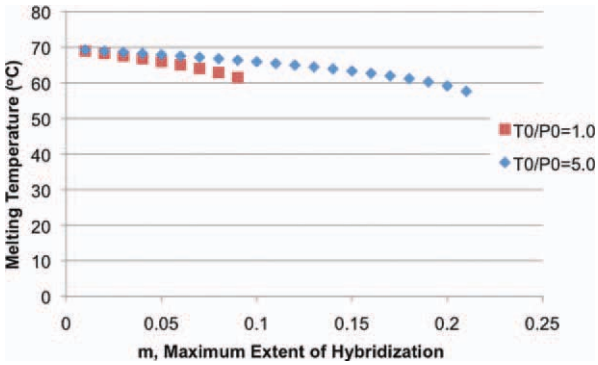

Figure 3. Trends in melting temperature with respect to maximum extent of hybridization at two different initial target-to-probe concentration ratios, 1.0 and 5.0 as extracted from Supporting Information Figure S3.

temperature (T^0_{hyb}) and the melting temperature (T_m). Expressions derived from Eq. 7 at these two temperatures can be equilibrated with respect to the standard Gibbs free energy change at the standard temperature. This yields an equation that demonstrates the relationship between the association equilibrium constants at the initial hybridization temperature and the melting temperature:

$$\ln\left(\frac{K_a(T_m)}{K_a(T^0_{hyb})}\right) = \frac{\Delta H^0_o}{R}\left(\frac{1}{T^0_{hyb}} - \frac{1}{T_m}\right) + \frac{\Delta C^0_p}{R}\ln\left(\frac{T_m}{T^0_{hyb}}\right) \quad (8)$$

Adding in the association equilibrium constant expressions at the initial hybridization and melting temperatures including the maximum extent of hybridization, m, and the initial target-to-probe concentration ratio (T_0/P_0) [Eq. 2 (at $\theta = 1$) and Eq. 3] and rearranging results in the final equation:

$$R\times\left[\ln\left(\frac{(1-m)\times(T_0/P_0 - m)}{(1-0.5m)\times(T_0/P_0 - 0.5m)}\times 0.5\right) - \frac{1}{R} \times\left(\frac{\Delta H^0_o}{T^0_{hyb}} - \Delta C^0_p \ln(T^0_{hyb})\right)\right] = \Delta C^0_p \ln(T_m) - \frac{\Delta H^0_o}{T_m} \quad (9)$$

where ΔH^0_o is the standard enthalpy change of coil-to-helix transition, ΔC^0_p is the specific heat capacity change, T^0_{hyb} is the initial hybridization temperature, and R is the universal gas constant.

The conditions imposed by this equation are:

$$(1)\ T_0/P_0 > m$$

$$(2)\ 0<m<1$$

To be able to use Eq. 9, one needs to know the standard enthalpy change of coil-to-helix transition on the surface, ΔH^0, at the reference state, the standard specific heat capacity change on the surface, ΔC^0_p, the maximum extent of hybridization, m, and initial target-to-probe ratio values, T_0/P_0. In solution, the standard enthalpy change of coil-to-helix transition of the authors duplex at 23°C is –209.4 kcal/mol, which is calculated using the Nearest-Neighbor method and the improved parameters of SantaLucia Jr et al.[7] The range of published values for specific heat capacity change is 7–332 cal/mol.bp.K in solution.[51] The following arguments are presented to substantiate the utilization of the respective standard enthalpy change of coil-to-helix transition and specific heat capacity change values.

The enthalpy change of transition represents how well the molecules interact in the two conformations. When one of the strands is immobilized on the surface, there is a considerable configurational entropy penalty imposed on the duplex formation in addition to the double-stranded structure with a stiff-backbone allowing a few conformations. According to a study by Watterson, the standard enthalpy change of coil-to-helix transition on the surface is decreased to a half or one-thirds of its value in solution.[40]

The specific heat capacity change represents the combined effect of solvent interactions (both solute–solvent and solvent–solvent), conformational entropy, electrostatics, and others with solvent effects being the most dominant. The presence of a surface and the decreased displacement of water during the transition can result in a smaller increase in the specific heat capacity compared to in-solution.[51] However, there are no studies that specifically look at the effect of surfaces on the specific heat capacity change.

Consequently, the following values of standard enthalpy change of coil-to-helix transition and specific heat capacity change are used to simulate the trend in T_m with respect to m and T_0/P_0 in Eq. 9: $\Delta H^0(23°C) = -104.7$ kcal/mol (half of the solution value), $\Delta C^0_p = 12.5$ cal/mol.bp.K (a value closer to the lower end of the range).

The authors main goal in this derivation is to observe the melting temperature behavior of a duplex with respect to different m and T_0/P_0 values. Using an initial hybridization temperature of 23°C and inserting the values above for the standard enthalpy change of transition and specific heat capacity change in Eq. 9, a surface plot can be drawn with respect to different initial target-to-probe concentration ratios and maximum extent of hybridization values to examine the behavior of T_m (Supporting Information Figure S3).

The effects of T_0/P_0 and m on T_m can be better observed with a more specific example. For this purpose, a cross-sectional cut of melting temperature change was extracted from Supporting Information Figure S3 at two T_0/P_0 values (1.0 and 5.0), and plotted with respect to different possible maximum extents of hybridization (Figure 3). The analysis was carried out based on the assumption that the probe concentration was the same in both.

For a constant probe density and probe concentration, an increase in the target concentration is expected to result in a higher m at the initial hybridization temperature with all other parameters being the same.[52,53] In the authors experiments, the actual value of m is unknown. However, the authors were able to make inferences from their PMT voltage values that resulted in near-saturation fluorescence intensities with different target concentrations at the initial hybridization temperature. Supporting Information Table 1 shows the related PMT voltages for Experimental Set 1, where the target concentration was varied from 0.5 to 15 nM with a constant probe amount of 0.82 pmol on 10^{18} Å^2 chip. Under these conditions, the PMT voltage values used to obtain the maximum dynamic range in detection increased accordingly with decreasing target concentration. The increase in PMT voltages, while maintaining the normalized average median intensity of the perfect-match signals at the initial hybridization temperature within the range of 58,000+/−1,100, proposes that there are fewer targets hybridizing with decreasing target concentration (lower m). Therefore, more PMT voltage is necessary to capture the highest intensity for the perfect-match probes without saturation.

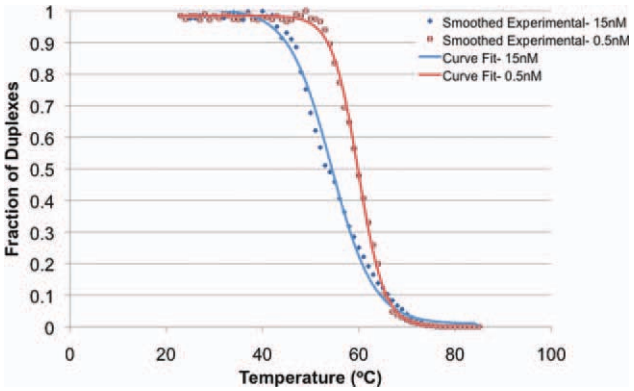

Figure 4. Experimentally observed melting curves of two duplexes formed on the surface with target concentrations of 15 and 0.5 nM and a probe amount of 0.82 pmol on a surface area of 10^{18} Å^2 (from Experimental Set 1).

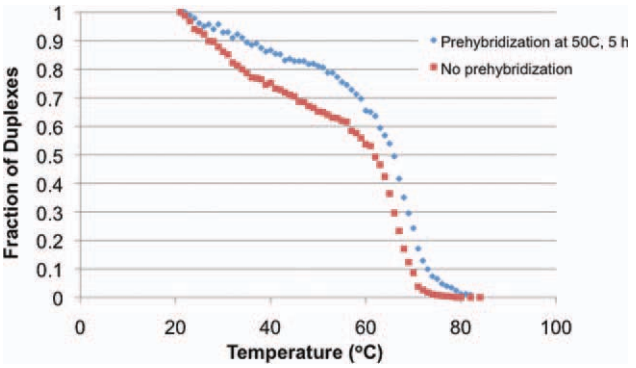

Figure 5. A representative (processed) perfect-match duplex melting curve and the effect of pre-hybridization at 50°C for 5 h observed in Experimental Set 3 with target concentration of 0.0165 nM and probe amount of 0.0165 pmol on a surface area of 10^{18} Å^2.

This means that in Figure 3, the low initial T_0/P_0 of 1.0 would have lower m. In this case, by looking at T_m trends for both initial target-to-probe concentration ratios in the same figure, the authors can conclude that the melting temperature of a duplex formed in the presence of lower target concentration could be higher than that formed with the higher target concentration. This inference from Figure 3, and in turn, Supporting Information Figure S3, supports the authors experimental finding that decreasing target concentration can lead to increasing T_m at a constant probe concentration and density for a duplex formed on the surface.

Alternatively, the resulting maximum extents of hybridization with higher target concentrations could lead to more surface hindrance due to increasing surface charge and crowding.[22] This can result in duplex denaturation occurring at lower temperatures than more stable duplexes on the surface as the melting progresses with increasing temperatures. Figure 4 demonstrates this phenomenon by two experimentally observed melting curves of duplexes formed with two different target concentrations (0.5 and 15 nM) at a constant probe amount (0.82 pmol on a surface area of 10^{18} Å^2; from Experimental Set 1). The curves were smoothed using the Savitzky–Golay method,[37] and fitted using the Boltzmann equation shown in Eq. 1. Duplexes start to melt at a lower temperature when the hybridization is performed with 15 nM of target concentration, and the shape of the melting curve also indicates its lower stability, with a less sharp transition demonstrating less temperature dependency.[38] On the other hand, the duplexes formed in the presence of a lower target concentration, 0.5 nM, prove to be more stable, and start to show observable denaturation at a higher temperature, and a sharper transition in the melting profile.

In another significant observation for increasing target concentration, the discrepancy between the predicted in-solution and observed on-surface T_ms also seems to increase at all probe concentrations. A target approaching the probe layer on the surface for hybridization may experience additional blocking on a microarray when compared with the in-solution hybridization reaction in which both strands are free to move and at comparably lower concentrations.[10,12,22] Due to increased crowding and lateral interactions between the probes and probe–target pairs in a denser layer on a microarray surface, the electrostatic hindrance of hybridization due to increasing surface charge, and the entropic hindrance due to the increased possibility of simultaneous binding of targets to multiple probes could be more prominent and inversely influence the stability of the helical structures formed. This might also explain the increasing discrepancy between the predicted in-solution and observed on-surface T_ms with increasing target concentrations as seen in the authors experiments.

Synthesis quality assessment using melting curves at very low target concentrations

Experimental Set 3 in Table 1 was designed to investigate the melting temperatures at very low initial target concentrations and probe amount on the surface. The target concentrations were 0.0165 and 0.027 nM, and the probe amount was kept constant at 0.0165 pmol on a surface area of 10^{18} Å^2. There were 145 probe synthesis spots on the chip.

The melting curves reproduced at these concentrations yielded distinctively different curves than the S-shaped curves observed in melting experiments with higher target concentrations and probe amounts (Supporting Information Figure S2 and Figure 5). The low temperature domain in these melting curves might be explained differently than the melting of a perfect-match pair at a higher temperature. A similar observation was made in studies on the single nucleotide polymorphism genotyping experiments by generating high-resolution melting curves in solution.[54,55] A mixture of heteroduplex (with single nucleotide polymorphism) and perfect-match (wild-type) samples is shown to reproduce melting curves with distinctive shapes in low temperature domains. With the presence of single base mismatch, the duplex with lower stability melts at a lower temperature than the perfect match; yielding a melting curve similar to the authors observations.

In our case, multiple melting processes in the low temperature domain of the melting curve could be one of the potential explanations. It may indicate the presence of sequences which form less stable duplexes than the perfect match itself: truncated or mismatch probe sequences, an inherent result of *in situ* oligonucleotide synthesis.[8] Using the step-wise synthesis yield, which is predicted to be 99.5% in the authors system, their 25-mer probes are expected to be 88% of the population in each spot; the rest of the probes in the population having a dispersion of shorter lengths with a distribution of lower Gibbs free energies in absolute value.[8]

To test their hypothesis of polydispersity in synthesized probe lengths and their melting, the authors tried to reduce the observed multi-melting process at the low temperature domain. The authors initially carried out the hybridization at a higher temperature of 50°C for 5 h, and then brought it down to the regular hybridization temperature of 23°C, and then continued hybridization until the equilibrium was reached. The 5 h hybridization time was determined by constantly monitoring the intensity of the spots for minimal change, indicating that equilibrium has been reached between the hybridization and melting reactions on the surface (3.5 h), and confirming it further with an additional 1.5 h observation. 50°C was chosen based on the profile observed without pre-hybridization by extracting a high enough temperature at which the multi-melting process seems to be completed. Figure 5 shows the effect of high temperature pre-hybridization for 5 h on the melting curve.

At high temperatures, the hybridization reaction could be favorable toward the more stable duplex, due to comparably lower association equilibrium constants of low stability duplexes.[9] After pre-hybridization at 50°C, as the temperature was decreased and hybridization was carried out at 23°C, there would be fewer targets in solution available for hybridization with the truncated probes, since perfect-match sequences are more stable and would retain more of the targets. This will result in a fewer number of duplexes formed with lower stabilities on the surface. As the melting experiment is carried out with increasing temperatures, the imperfect duplexes, which are now fewer in number, would melt in the low temperature domain of the melting curve; but the slope of the curve in this region would indicate a smoother transition than the case without any high temperature pre-hybridization. The behavior of the data shown seems to be in agreement with this potential explanation.

Conclusion

In this study, the dependence of DNA melting temperature on target concentration on an oligonucleotide microarray surface was examined. A novel automated experimental system capable of real-time equilibrium monitoring of the melting of DNA duplexes on microfluidic oligonucleotide arrays was developed. This set-up was utilized to create melting profiles of a 25-mer perfect-match probe–target pair at different target concentrations and probe amounts. It was observed that the melting temperature decreases on the surface with respect to in-solution, which is consistent with various published studies concluding that more electrostatic and entropic restrictions could be imposed on the double helix structure by the presence of a denser, impenetrable, and charged surface layer.

It was also interestingly seen in the authors experiments that at constant probe amounts, an increasing target concentration trend was accompanied with decreasing melting temperature. This is an opposite trend to what is expected in the solution and gel-based arrays, but in agreement with various models and simulations in the published reports. As a result of a higher probability of target binding to more than one probe with increasing target concentration as well as the additional electrostatic and entropic penalties imposed on the structure, melting duplexes appear to exhibit lower melting temperatures at higher target concentrations. For similar reasons, an increasing discrepancy between the in-solution predicted and on-surface observed melting temperatures can be expected with increasing target concentrations. With the introduction of the maximum extent of hybridization term, m, the modification of the equilibrium constant expressions at the melting and initial hybridization temperatures and the temperature dependent van't Hoff equation, the authors were able to graphically demonstrate that it is possible to observe decreasing melting temperatures with increasing target concentrations at surface-adapted standard enthalpy change of transition and specific heat capacity change values for duplex formation.

These findings could aid in further development and understanding of microarrays. It has been experimentally demonstrated in this article that lower target concentrations can result in higher melting temperatures. With this knowledge in mind, when a small amount of target is available for analysis, informed decisions about hybridization conditions could potentially reduce false negatives.[16] There are several other potential areas in which this experimental system could be utilized. For example, similar to high-resolution melting method in solution,[54,55] mutation scanning, and SNP detection in parallel could be explored by creating and monitoring the melting curves on the surface and comparing them against several reference curves. In addition, similar to the in-solution model by SantaLucia Jr et al.,[7] a Nearest-Neighbor model can be proposed for on-surface applications to calculate the thermodynamic parameters for DNA helix-to-coil transitions and to predict the DNA melting temperature using the estimates of various base-pair combinations at equilibrium on the surface. Further studies may also include introducing various types of mismatches at different positions on the probes and/or the targets, investigating the effects of probe and/or target lengths, and analyzing a real gene in this system.

Experiments performed with low target concentrations and probe amounts yielded melting curves different than what was seen with high target concentrations and probe amounts. A possible multiple melting process was observed in the low temperature domain of the curves. This could be associated with the polydispersity of the probe length on the surface due to the truncated sequences, which is an inherent characteristic of *in situ* combinatorial oligonucleotide synthesis on the surface. These sequences exhibit lower stability than the perfect match probes, resulting in them melting at lower temperatures than the perfect-match. This hypothesis was further tested with pre-hybridization experiments at a higher temperature, and supporting results were observed. This approach can play its role as an important tool to further assess the quality of the probes synthesized on the surface.

The experimental and theoretical approaches presented in this study can be utilized to further analyze different systems and surface parameters, to assess the optimum hybridization conditions to minimize false positive and negative signals, as well as to improve the reliability, reproducibility, and accuracy of the results obtained. Conventional microarray systems aim to detect the target capture in steady-state at a single data point. Including a real-time monitoring system can assist in recording the kinetics of hybridization and determining the thermodynamics of the reaction on the surface. Furthermore, an addition of a microfluidics component in a closed system can also provide faster hybridization times, and within the optimized conditions, higher signal-to-noise ratios, broader dynamic range, and possibly smaller estimation errors.[56,57]

Finally, the experimental system can be modified to include an in-line real-time detection system to monitor the fluorescence intensity change in solution during the hybridization reaction on the surface. This could allow for subsequent analysis to calculate the maximum extent of hybridization, m, and the surface coverage as DNA melting proceeds at increasing temperatures. Furthermore, by detecting the target concentration changes in the solution as well as the signal intensity changes on the surface during hybridization, the kinetics of hybridization can be modeled more accurately under the given conditions.

Acknowledgment

The authors would like to thank Dr. Zhishan Hua and Mr. Yusuf E. Murgha for their contributions. This work was supported by grants from National Institute of Health [1R41HG004103-01, 1R21HG003725-01, 1R01 GM068564-01].

Literature Cited

1. Anguiano A, Nevins J, Potti A. Toward the individualization of lung cancer therapy. *Cancer* 2008;113:1760–1767.
2. Cogburn L, Wang X, Carre W, Rejto L, Aggrey S, Duclos M, Simon J, Porter T. Functional genomics in chickens: development of integrated-systems microarrays for transcriptional profiling and discovery of regulatory pathways. *Comp Funct Genomics* 2004;5:253–261.
3. Conejero-Goldberg C, Wang E, Yi C, Goldberg T, Jones-Brando L, Marincola F, Webster M, Torrey E. Infectious pathogen detection arrays: viral detection in cell lines and postmortem brain tissue. *Biotechniques* 2005;39:741–751.
4. Hughes M, Deharo L, Pulivarthy S, Gu J, Hayes K, Panda S, Hogenesch J. High-resolution time course analysis of gene expression from pituitary. *Cold Spring Harb Symp Quant Biol* 2007;72:381–386.
5. Milano A, Pendergrass S, Sargent J, George L, McCalmont T, Connolly M, Whitfield M. Molecular subsets in the gene expression signatures of scleroderma skin. *PLoS One* 2008; 3:e2696.
6. Owczarzy R, You Y, Moreira B, Manthey J, Huang L, Behlke M, Walder J. Effects of sodium ions on DNA duplex oligomers: improved predictions of melting temperatures. *Biochemistry* 2004;43:3537–3554.
7. SantaLucia J Jr, Allawi H, Seneviratne P. Improved nearest-neighbor parameters for predicting DNA duplex stability. *Biochemistry* 1996;35:3555–3562.
8. Forman J, Walton I, Stern D, Rava R, Trulson M. Thermodynamics of duplex formation and mismatch discrimination on photolithographically synthesized oligonucleotide arrays. In: Leontis NB, SantaLucia J Jr, editors. *ACS Symposium Series – Molecular Modeling of Nucleic Acids*. Washington, DC: American Chemical Society; 1998:206–228.
9. Glazer M, Fidanza J, McGall G, Trulson M, Forman J, Suseno A, Frank C. Kinetics of oligonucleotide hybridization to photolithographically patterned DNA arrays. *Anal Biochem* 2006;358: 225–238.
10. Halperin A, Buhot A, Zhulina E. Brush effects on DNA chips: thermodynamics, kinetics, and design guidelines. *Biophys J* 2005;89:796–811.
11. Schmitt T, Knotts T IV. Thermodynamics of DNA hybridization on surfaces. *J Chem Phys* 2011;134:205105.
12. Shchepinov M, Case-Green S, Southern E. Steric factors influencing hybridisation of nucleic acids to oligonucleotide arrays. *Nucleic Acids Res* 1997;25:1155–1161.
13. Horne M, Fish D, Benight A. Statistical thermodynamics and kinetics of DNA multiplex hybridization reactions. *Biophys J* 2006;91:4133–4153.
14. Sartor M, Schwanekamp J, Halbleib D, Mohamed I, Karyala S, Medvedovic M, Tomlinson C. Microarray results improve significantly as hybridization approaches equilibrium. *Biotechniques* 2004;36:790–796.
15. Wang Y, Miao Z, Pommier Y, Kawasaki E, Player A. Characterization of mismatch and high-signal intensity probes associated with Affymetrix genechips. *Bioinformatics* 2007;23: 2088–2095.
16. Bhanot G, Louzoun Y, Zhu J, DeLisi C. The importance of thermodynamic equilibrium for high throughput gene expression arrays. *Biophys J* 2003;84:124–135.
17. Wick N, Bruck J, Gurnhofer E, Steiner C, Giovanoli P, Kerjaschki D, Thurner S. Nonuniform hybridization: a potential source of error in oligonucleotide-chip experiments with low amounts of starting material. *Diagn Mol Pathol* 2004;13: 151–159.
18. Peplies J, Glockner F, Amann R. Optimization strategies for DNA microarray-based detection of bacteria with 16S rRNA--targeting oligonucleotide probes. *Appl Environ Microbiol* 2003; 69:1397–1407.
19. Yatsenko S, Shaw C, Ou Z, Pursley A, Patel A, Bi W, Cheung S, Lupski J, Chinault A, Beaudet A. Microarray-based comparative genomic hybridization using sex-matched reference DNA provides greater sensitivity for detection of sex chromosome imbalances than array-comparative genomic hybridization with sex-mismatched reference DNA. *J Mol Diagn* 2009;11:226–237.
20. Allen J, Schoch E, Stubbs J. Effect of surface binding on heterogeneous DNA melting equilibria: a Monte Carlo simulation study. *J Phys Chem B* 2011;115:1720–1726.
21. Ambia-Garrido J, Vainrub A, Montgomery Pettitt B. Free energy considerations for nucleic acids with dangling ends near a surface: a coarse grained approach. *J Phys Condens Matter* 2011;23:325101.
22. Binder H. Thermodynamics of competitive surface adsorption. *J Phys Condens Matter* 2006;18:491–532.
23. Fuchs J, Dell'Atti D, Buhot A, Calemczuk R, Mascini M, Livache T. Effects of formamide on the thermal stability of DNA duplexes on biochips. *Anal Biochem* 2010;397:132–134.
24. Fuchs J, Fiche J, Buhot A, Calemczuk R, Livache T. Salt concentration effects on equilibrium melting curves from DNA microarrays. *Biophys J* 2011;99:1886–1895.
25. Hooyberghs J, Van Hummelen P, Carlon E. The effects of mismatches on hybridization in DNA microarrays: determination of nearest neighbor parameters. *Nucleic Acids Res* 2009;37:e53.
26. Irving D, Gong P, Levicky R. DNA surface hybridization: comparison of theory and experiment. *J Phys Chem B* 2010; 114:7631–7640.
27. Naiser T, Kayser J, Mai T, Michel W, Ott A. Stability of a surface-bound oligonucleotide duplex inferred from molecular dynamics: a study of single nucleotide defects using DNA microarrays. *Phys Rev Lett* 2009;102:218301.
28. Peterson A, Heaton R, Georgiadis R. The effect of surface probe density on DNA hybridization. *Nucleic Acids Res* 2001;29: 5163–5168.
29. Vainrub A, Pettitt B. Surface electrostatic effects in oligonucleotide microarrays: control and optimization of binding thermodynamics. *Biopolymers* 2003;68:265–270.
30. Tan P, Downey T, Spitznagel E Jr, Xu P, Fu D, Dimitrov D, Lempicki R, Raaka B, Cam M. Evaluation of gene expression measurements from commercial microarray platforms. *Nucleic Acids Res* 2003;31:5676–5684.
31. Jayaraman A, Hall C, Genzer J. Computer simulation study of probe-target hybridization in model DNA microarrays: effect of probe surface density and target concentration. *J Chem Phys* 2007;127:144912.
32. Moreira B, You Y, Behlke M, Owczarzy R. Effects of fluorescent dyes, quenchers, and dangling ends on DNA duplex stability. *Biochem Biophys Res Commun* 2005;327:473–484.
33. Branham W, Melvin C, Han T, Desai V, Moland C, Scully A, Fuscoe J. Elimination of laboratory ozone leads to a dramatic improvement in the reproducibility of microarray gene expression measurements. *BMC Biotechnol* 2007;7:8.
34. Mandal S, Rouillard J, Srivannavit O, Gulari E. Cytophobic surface modification of microfluidic arrays for in situ parallel peptide synthesis and cell adhesion assays. *Biotechnol Prog* 2007;23:972–978.

35. Gao X, LeProust E, Zhang H, Srivannavit O, Gulari E, Yu P, Nishiguchi C, Xiang Q, Zhou X. A flexible light-directed DNA chip synthesis gated by deprotection using solution photogenerated acids. *Nucleic Acids Res* 2001;29:4744–4750.
36. Wick L, Rouillard J, Whittam T, Gulari E, Tiedje J, Hashsham S. On-chip non-equilibrium dissociation curves and dissociation rate constants as methods to assess specificity of oligonucleotide probes. *Nucleic Acids Res* 2006;34:e26.
37. Owczarzy R. Melting temperatures of nucleic acids: discrepancies in analysis. *Biophys Chem* 2005;117:207–215.
38. Mergny J, Lacroix L. Analysis of thermal melting curves. *Oligonucleotides* 2003;13:515–537.
39. Southern E, Mir K, Shchepinov M. Molecular interactions on microarrays. *Nat Genet.* 1999;21:5–9.
40. Watterson J, Piunno P, Wust C, Krull U. Effects of oligonucleotide immobilization density on selectivity of quantitative transduction of hybridization of immobilized DNA. *Langmuir* 2000;16:4984–4992.
41. Marky L, Breslauer K. Calculating thermodynamic data for transitions of any molecularity from equilibrium melting curves. *Biopolymers* 1987;26:1601–1620.
42. Fotin A, Drobyshev A, Proudnikov D, Perov A, Mirzabekov A. Parallel thermodynamic analysis of duplexes on oligodeoxyribonucleotide microchips. *Nucleic Acids Res* 1998;26:1515–1521.
43. Zlatanova J, Mirzabekov A. Gel-immobilized microarrays of nucleic acids and proteins. Production and application for macromolecular research. *Methods Mol Biol* 2001;170:17–38.
44. Georgiadis R, Peterlinz K, Peterson A. Quantitative measurements and modeling of kinetics in nucleic acid monolayer films using SPR spectroscopy. *J Am Chem Soc* 2000;122:3166–3173.
45. Gong P, Levicky R. DNA surface hybridization regimes. *Proc Natl Acad Sci U S A.* 2008;105:5301–5306.
46. Tawa K, Knoll W. Mismatching base-pair dependence of the kinetics of DNA–DNA hybridization studied by surface plasmon fluorescence spectroscopy. *Nucleic Acids Res* 2004;32:2372–2377.
47. Wong I, Melosh N. An electrostatic model for DNA surface hybridization. *Biophys J* 2010;98:2954–2963.
48. Halperin A, Buhot A, Zhulina E. On the hybridization isotherms of DNA microarrays: the Langmuir model and its extensions. *J Phys Condens Matter* 2006;18:5463–5490.
49. Smith J, Van Ness H, Abbott M. *Introduction to Chemical Engineering Thermodynamics*, 5th ed. New York: McGraw Hill, Inc.; 1996.
50. Holbrook J, Capp M, Saecker R, Record M Jr. Enthalpy and heat capacity changes for formation of an oligomeric DNA duplex: interpretation in terms of coupled processes of formation and association of single-stranded helices. *Biochemistry* 1999;38:8409–8422.
51. Mikulecky P, Feig A. Heat capacity changes associated with nucleic acid folding. *Biopolymers* 2006;82:38–58.
52. Wu L, Thompson D, Li G, Hurt R, Tiedje J, Zhou J. Development and evaluation of functional gene arrays for detection of selected genes in the environment. *Appl Environ Microbiol* 2001;67:5780–5790.
53. Yin H, Cao L, Qiu G, Wang D, Kellogg L, Zhou J, Dai Z, Liu X. Development and evaluation of 50-mer oligonucleotide arrays for detecting microbial populations in Acid Mine Drainages and bioleaching systems. *J Microbiol Methods* 2007;70:165–178.
54. Gundry C, Vandersteen J, Reed G, Pryor R, Chen J, Wittwer C. Amplicon melting analysis with labeled primers: a closed-tube method for differentiating homozygotes and heterozygotes. *Clin Chem* 2003;49:396–406.
55. Liew M, Pryor R, Palais R, Meadows C, Erali M, Lyon E, Wittwer C. Genotyping of single-nucleotide polymorphisms by high-resolution melting of small amplicons. *Clin Chem* 2004;50:1156–1164.
56. Chung Y, Lin Y, Shiu M, Chang W. Microfluidic chip for fast nucleic acid hybridization. *Lab Chip* 2003;3:228–233.
57. Peytavi R, Raymond F, Gagne D, Picard F, Jia G, Zoval J, Madou M, Boissinot K, Boissinot M, Bissonnette L, Ouellette M, Bergeron M. Microfluidic device for rapid (<15 min) automated microarray hybridization. *Clin Chem* 2005;51:1836–1844.

Manuscript received Aug. 20, 2011 and revision received Nov. 8, 2011.